Structural and Magnetic Properties of Copper Substituted Mg-Ferrites

Tatiana Kiseleva[1], Vladislav Kabanov[1], Alexander Ilyushin[1,2], Gennadiy Markov[3], Deleg Sanga[4] and H. Hirazawa[5]

[1]Moscow M.V.Lomonosov State University, Physics Faculty, Mocow, Russia
[2]The Ibragimov Complex Institute, RAS, Grozniy, Russia
[3]The Schmidt Institute of Physics of the Earth RAS, Moscow, Russia
[4]Institute of Physics and Technology, Mongolian Academy of Science, Ulan Bator, Mongolia
[5]National Technological Institute, Ehime, Japan

Abstract. Polycrystalline ferrite powders of $Mg_{1-x}Cu_xFe_2O_4$ (x = 0.2, 0.4, 0.6, 0.8, 1) system synthesized by ceramic technology have been investigated. Samples showed the non-monotonic dependency of heat generation effect in AC magnetic field with increasing concentration of copper. To reveal peculiarities of the structural and magnetic state of the samples and their influence on the heat generation ability we performed a complex study, including X-ray diffractometry, Mössbauer spectroscopy, Scanning electron microscopy, measurements of temperature dependencies of susceptibility and saturation magnetization, hysteresis parameters and FORC.

Typical ferrimagnetic character with small coercivity and saturation magnetization was found. We carried out that anomalous influence of Cu^{2+} ion substitution respectively to the $Mg_{1-x}Cu_xFe_2O_4$ ferrite powder manifested in heat generation ability rise up to x=0.6. The subsequent sharp reducing of this characteristic were accompanied by the main phase crystal structure distortion followed by phase separation to cubic and tetragonal structure. This was matched by in an increase of ferrite particles crystallite size and size distribution appearance. The saturation magnetization and Curie temperature dependencies observed for powders via Cu substitution was explained by phase composition, the cations distributions between ferrite sublattices, modulation of exchange interaction.

1 Introduction

The new opening opportunities for ferrite's systems applications in different fields of modern industry (catalysis, adsorption, humidity sensors, ferrofluids and ferroelastomers technology, components of health monitoring systems and medicine) require the involvement of modern and powerful experimental techniques. The properties-structure-sizes interdependence study allows to manage ferrite's functionality [1-3]. Among a number of industrial important ferrite compositions magnesium ferrite ($MgFe_2O_4$) particles have favorable magnetic properties and biological compatibility. It is worth mentioning that $MgFe_2O_4$ particles of micrometer-range sizes are reported to exhibit greater magnetic heating than do other ferrites [4-5], but a lot of afforts have veen made to synthesize and research these compounds in nanoparticulate form. Despite a lot of efforts to modulate specific magnetic properties of this ferrite as by types of substituting metals and their combinations, included in composition, the cationic distribution and interaction between them, as particles' sizes distributions, the issue of the best composition of ferrite particles to obtain effective heating abilities under application of alternating magnetic field remains controversial [6-7]. The investigation of the different effects influence on the properties of ferrites, which are used as components of complex composite systems for the purposes of therapeutic implants, seems to be important.

It is known, that ferrites have the general formula $(M_{1-z}Fe_z)[M_zFe_{2-z}]O_4$. The divalent metal atoms M (Mg, Fe, Cu or mixture of them) can occupy either eight tetrahedral (A) or sixteen octahedral [B] sites of a cubic mineral spinel structure as depicted by the parentheses or brackets, respectively, z represents the degree of inversion. The complexity of the above formula and the nature of preparation techniques strongly suggest a variation in unit cell composition and possibly a variation in the arrangement of Mg^{2+} and Fe^{3+} ions over the available tetrahedral and octahedral sites. Depending on the cations distribution in (A) and [B] sites, two extreme states—normal (z = 0) and inverse (z = 1) or an intermediate mixed state may be realized. Ultimate magnesium ferrite ($MgFe_2O_4$) is an inverse spinel taken to be collinear ferrimagnetic [8,9], whose degree of inversion depends on the synthesis temperature and cooling rate [8,10]. The ultimate copper ferrite ($CuFe_2O_4$) exists in tetragonal and cubic structures [10]. The distortions from one structure to another is directly related to the magnetic properties. The cubic structure posesses a larger magnetic moment than that of the tetragonal one, because there are more cupric ions (Cu^{2+}) at tetrahedal sites in cubic structure as compared to that in the case of tetragonal structure. As the ionic radii of the Fe, Mg and Cu cations (the ionic radius of Cu^{2+}(0.85

* Corresponding author: Kiseleva.TYu@gmail.com

Å) Mg^{2+}(0.78 Å) (Fe^{2+}(0.83 Å) Fe^{3+}(0.77 Å) Mg^{2+}(0.78 Å) Fe^{2+}(0.83 Å) Fe^{3+}(0.77 Å) are not quite different, random occupancy of cations in any site is possible and will also leads to produce several structural and hyperfine effects that may reveal modulation of ferrite magnetic properties.

The aim of this works was to investigate the practically important structure and magnetic properties correlations in $Mg_{1-x}Cu_xFe_2O_4$ samples series for varying Cu-substitution ($0<x<1$).

2 Experimental

Polycrystalline ferrite powders of $Mg_{1-x}Cu_xFe_2O_4$ (x = 0.2, 0.4, 0.6, 0.8, 1) system were synthesized by ceramic technology at 1473 K [6].

X-ray diffraction (XRD) has been performed on Empyrean (PAnalytical) diffractometer equipped with a PIXcel3D detector (Bragg-Brentano geometry, CuK_α radiation, Ni filter). ISCD database was used for phase identification. Quantitative phase analysis was carried out using the Rietveld refinement method with derivative difference minimization applying HighScore software.

Scanning electron microscopy (SEM) images of samples have been obtained using Quanta 3D FEG (FEI) microscope.

Fe^{57} Mössbauer study of structure and magnetic state of samples was carried out at 80 and 300 K with ^{57}Co(Rh) source. Analysis of the spectra have been performed with UnivemMS software. All spectra were referenced to α-Fe at room temperature.

Temperature generation ability of ferrites in AC (370kHz, 1.50kA/m) magnetic field was measured on laboratory equipment with IR-thermometer [7].

Hysteresis loops and FORC (first-order-reversal-curves) diagrams were measured at room temperature in applied magnetic fields up to 10 kOe using VSM 3900 magnetometer (LakeShore), temperature dependencies of saturation magnetization and susceptibilities were measured using Curie balance (Ltd "Orion") in temperature range 293-1073 K in applied magnetic field of 4,5 kOe, and Cappabridge MFK-1FA (AGICO) in magnetic field 200 A/m and frequency ~1000 Hz, correspondingly.

3 Results and discussion

Plot of the temperature enhancement from room temperature (ΔT) for powders in the AC(370kHz, 1.50kA/m) magnetic field (Fig.1, a) shows that heat generation ability was improved with increasing the Cu substitution, the highest heat generation ability ($\Delta T \approx 37^o$) was obtained at x=0.6. Then, the heat generation ability abruptly decreases and lost over x=1.0. Similar nonmonotoneous dependencies were observed for other ferrite compositions synthesized by the same technology and had different degree of heat generation. In order to gain more information regarding the structure and properties correlations in our synthesized $Mg_{1-x}Cu_xFe_2O_4$ powders we have undertaken X-ray diffraction, Moössbauer spectroscopy and complex magnetic properties study.

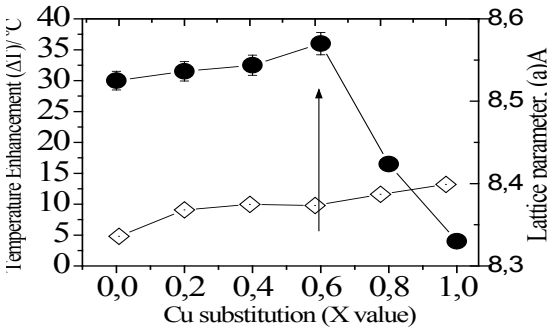

Fig.1. Temperature generation ability of ferrites in AC (370kHz, 1.50kA/m) magnetic field (circles) and lattice parameter (rhombuses) via Cu substitution in $Mg_{1-x}Cu_xFe_2O_4$.

The X-ray diffraction patterns of $Mg_{1-x}Cu_xFe_2O_4$ ferrite system for x=0-1.0 (samples 1-6) analysis revealed the polycrystalline structure with μm-sized crystallites. The main phase in all samples is *f*cc (cubic) spinel. Several additional impurities of crystalline phases (MgO, Fe_2O_3, $CuFeO_3$) were identified as a reaction by-products. For the ultimate Cu-substitution (x=1) the appearing of tetragonal ferrite structure in a very small amount have been determined. Lattice parameter of the cubic phase increases with Cu^{2+} content with small distortion from the linear dependence at x=0.4-0.6 (Fig.1, a). The dependence of the integrated intensity ratio $I(220)/I(222)$ on the Cu content revealed that there is a cations redistribution between (*A)* and [*B*] sites.

Fig.2 shows the concentration variation of Mössbauer spectra, measured at 300K. The spectra indicate a magnetic ordering with spectral lines broadening via Cu-substitution. Mössbauer spectra analysis allowed to resolve at first exact phase composition: Fe_2O_3 ,$CuFeO_3$, Cu(Fe) phases additionally to the main spinel phase have been determined for x=0 and x=1, correspondingly. Then, spectra profile fitting in a simple model resolving (*A*) and [*B*] subspectra due to iron atoms in the two sublattices was applied. Mossbauer spectrum of $MgFe_2O_4$ is known to have an asymmetric broadening of the [*B*]-site lines indicating the presence of several subpatterns arising from the different possible nearest-neighbor (*A*)-site configurations via supertransfer mechanism [9]. According to [11] the more covalent character of the Fe(*A*) –O bond compared to the Fe[*B*] –O bond explains qualitatively why the spin-density transfer from (*A)* to [*B]* in the spinel structure is more effective than vice versa. As a consequence, the (A)-site lines usually do not show any structure that indicates the presence of a narrower hyperfine field's distribution. Mössbauer spectra parameters resolved from fitting allowed to determine the concentration dependencies of hyperfine magnetic fields on Fe^{57} atoms in different sublattices so as an inversion degree (z) changes.

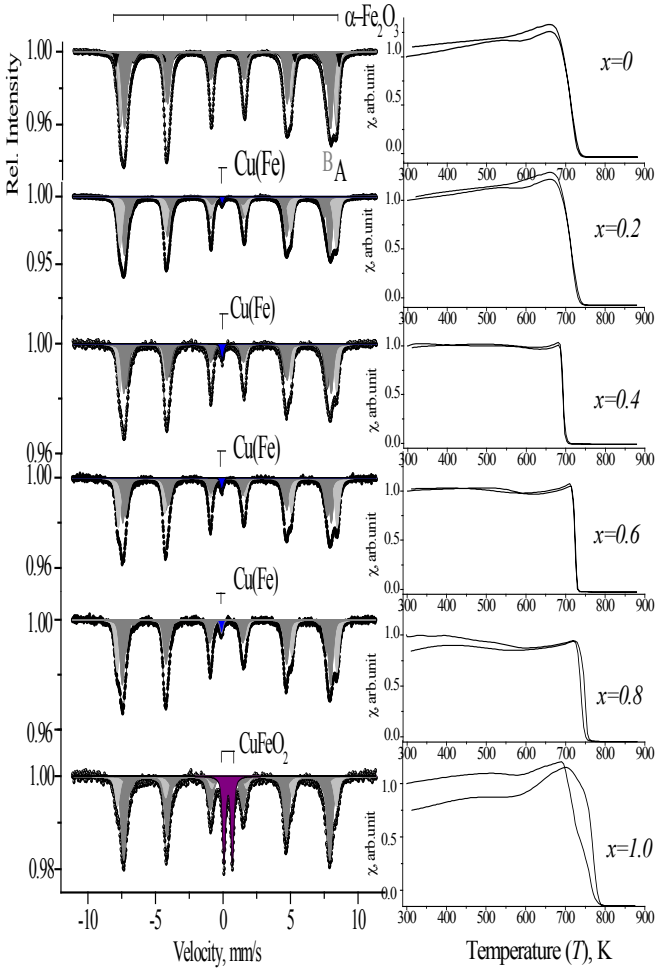

Fig.2. Mossbauer spectra at 300 K (left panel) and temperature dependence of susceptibility (right panel) in dependence on Cu substitution correspondingly)

The degree of inversion was calculated from the subspectral areas (I(A)/I(B)=*f*(A)/*f*(B)*z/(2-*z*)), assuming that the ratio of the recoilless fractions is *f*(B)/*f*(A)=0.94 at room temperature. The resulting composition dependence of inversion degree plotted on Fig.3 demonstrates the changes at *x*=0.4-0.6.

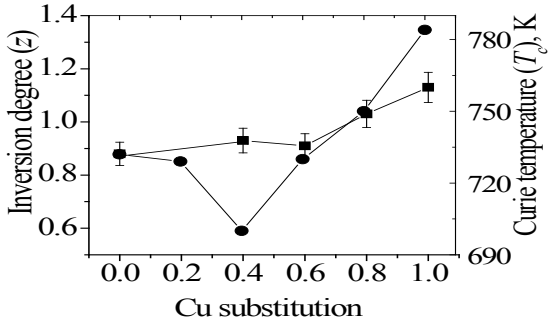

Fig.3. Inversion degree (z) (squares) and Curie temperature (Tc) (circles) dependencies vs Cu substitution

Fig.2 (right panel) shows the temperature dependence of susceptibility χ(T) for samples. The results exhibit normal ferrimagnetic behavior. The pure sample corresponds to *x*=0.2-0.8 and in accordance with XRD and Mössbauer phase analysis data. The ultimate ferrite sample with *x*=1 demonstrated multiphase behavior. The Curie temperature (*Tc*) obtained from susceptibility data is shown in Fig.3.

The Curie temperature (T_c) of the main phase in the ferrite samples measured from χ(T) curves has nonmonotonic dependence via Cu substitution: gradual decrease of the Tc value to the sample with x = 0.4 and followed by an Tc increase. It is known that Tc is determined by the overall strength of the intersublattice AB interactions, but sometimes the intrasublattice AA and BB interactions may become important. The decrease in Tc with increasing concentration of Cu may be explained by the modification of A-B exchange interaction strength due to the change of cations distribution between A and B sites.

Hysteresis loops *J*(H) for $Mg_{1-x}Cu_xFe_2O_4$ ferrite samples (Fig.4) showed nonmonotonic dependence: it is divided into three groups: I (*x*=0-0.2, curves 1,2); II (*x*=0.8-1, curves 5,6); III (*x*=0.4-0.6, curves 3,4). Similar non-monotonic behavior of hysteresis loops has been reported in several works subjected to study of substitution influence [12]. Magnetic parameters determined from the curves were analysed and plotted in as a Day's diagram [13-14] (J_{rs}/J_s vs H_{cr}/H_c) (Fig.5, a). This diagram clearly demonstrated the three ranges that correspond to different sizes or domain state in the particles: I - the smallest particles are probably a mixture of SD (single domain) and PSD (pseudo single domain) particles, II - larger particles are mixture PSD and MD (multi domain) particles, III - the largest particles (multi-domain state of ferrite powders).

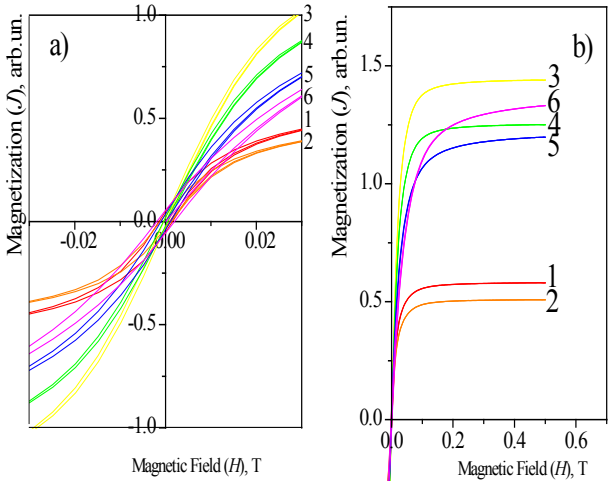

Fig.4. Hysteresis loops vs Cu substitution in small fields (a) and in high fields (b) for $Mg_{1-x}Cu_xFe_2O_4$ (*x*=0-1, marked 1-6, correspondingly)

Much more detailed information about magnetic assemblages than standard hysteresis curves was derived from the measured FORC (first-order-reversal-curves) diagrams. Characteristic FORC diagram for the samples with concentrations that fall within the determined

ranges are shown on (Fig 5 b, c, d). FORC was able to detect the coercive force distribution as well as the magnetic interactions within particles assemblage [15].

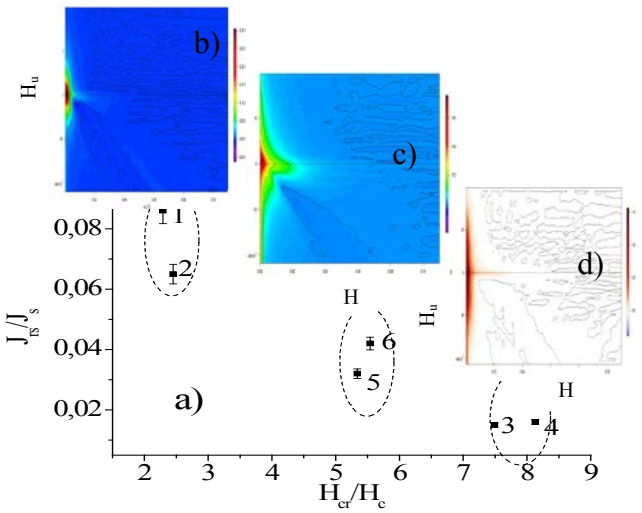

Fig.5. Day's diagram (a), typical FORC diagram for corresponding samples groups (b,c,d)

FORC diagrams were measured by saturating a sample in VSM magnetometer in a field H_{sat}, decreasing the field to a reversal field H_a, then sweeping the field back to H_{sat} in a series of regular field steps H_b as illustrated in color on Fig.5 (b,c,d). This process is repeated for many values of H_a yielding a series of FORCs, and the measured magnetization at each step as the function of H_a and H_b gives $J(H_a, H_b)$. The FORC distribution $\rho(H_a, H_b)$ is defined as the mixed second derivative of the interaction surface.

For each sample we determined the main FORC peak, which is the coercivity field corresponding to the maximum of the FORC distribution (plotted on Fig.5 as $H_u=(H_a+H_b)/2$, $H=(H_b-H_a)/2$). The interaction field is quantified with the full width at half-maximum of the main peak of the FORC distribution parallel to the abscissa axis through the maxima peak H. It was revealed from FORC diagram that for x=0.4-0.6 large multidomain particles were synthesized; the smallest particles sizes corresponds to x=0-0.2 ; intermediate for x=0.8-1. This fact was confirmed by SEM imaging (Fig.6, a,b,c) of particles with restoration of particles sizes distribution (Fig.6, d) where they measured from a few to several tens of microns. Cu substitution tends to increase particles sizes.

The decrease of H_c is in accordance with the increase of average particle's size and the immoderate nonmagnetic ions entering into the lattice that may result in the energy reduction of magneto-crystalline anisotropy that leads to the resulting heat generation ability.

Summary

Synthesized by ceramic technology at 1473 K polycrystalline $Mg_{1-x}Cu_xFe_2O_4$ ferrite powders were investigated by structural and magnetic methods. The effect of Cu-substitution (x=0, 0.2, 0.4, 0.6, 0.8, 1) was investigated. To sum up the results we found that:

1)Synthesized ferrites demonstrated anomalous heating ability via Cu substitution that is connected with their structural and magnetic properties variation.

2) All samples demonstrated soft magnetic behaviour with coercivity depending on particles sizes and domain state.

3) Magnetic hyperfine interaction measured by Mossbauer spectrometry showed that Cu^{2+} has an appreciable effect on the magnetic field of the octahedral sites.

4) It was determined that magnetic properties of synthesized ferrites are in accordance with particles sizes and cations distribution.

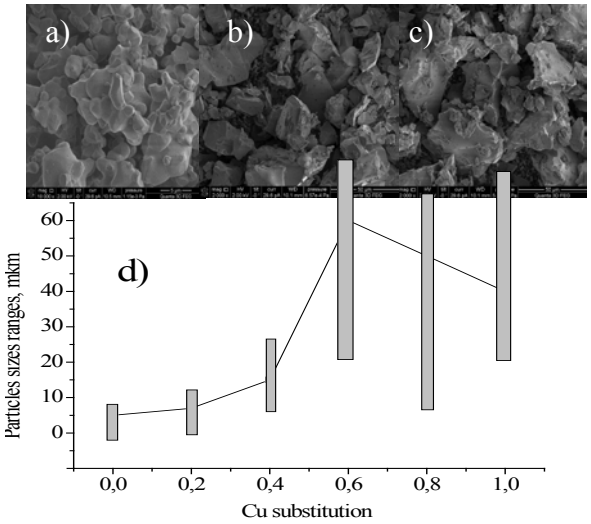

Fig.6. SEM images for x=0 (a), 0.4 (b) and 0.8 (c) and particles sizes distributions (d) from SEM images analysis via Cu substitution

Acknowledgments

Authors thank Moscow University Program of Development and the Ministry of education and science of the Russian Federation (grant 14.Z50.31.0017) for technical and financial support.

References

1. S. Kumar, A. Daverey, et.al, J. Mater. Chem. **B**(1) 3652 (2013)
2. E.A. Schultz-Sikma, H.M. Joshi, et al. , Chem. Mater. **23** (10) 2657–2664 (2011)
3. A.Yu. Zubarev, A.S. Elkady, Physica **A** 413400–408 (2014)
4. T. Maehara, K. Konishi, et al., Jpn. J. Appl. Phys. **41** 1620–1621 (2002)
5. T.Maehara, K.Konishi et al. , J. of Materials Science **40**, 135-138 (2005)
6. H.Hirazawa et.al. , J. of Alloys and Comp., **461**, 467-471 (2008)
7. Hirazawa H., Ito Y., Sangaa D., AIP Conference Proceed. **1763**, 020009 (2016)

8. M.R. Barati, C.Selomulya, J. of Appl.Phys. **115** 17B522 (2014)
9. G. A. Sawatsky, F. Van Der Woude, *Phys.Rev.* **187** 2, 747-757 (1969)
10. J. Smit and H. P. J. Wijn, "*Ferrites*," John Wiley & Sons Inc. New York, (1959)
11. F. Van Der Woude and G. A. Sawatzky, Phys. Rev. B **4**, 3159 (1971)
12. P.K. Roy and J.Bera, J.Magn.Magn.Mater **298** 38 (2006)
13. R.Day, M.Fuller, Phys. Earth Planet. Inter., **13**, 260—267 (1977)
14. D.J.Dunlop J. Geophys. Res. S Solid Earth, 107, B3, 2046—2067 (2002)
15. A.R.Muxworthy, A.P. Roberts First-order reversal curve (FORC) diagrams, in *Encyclopedia of Geomagnetism and Paleomagnetism*, Springer, NY (2006)